CALCULATION OF SUB-BANDS {1,2,5,6} FOR 64-POINT COMPLEX FFT AND ITS EXTENSION TO N ($= 2^N$)-POINT FFT

Bhaskar Sen

Independent Researcher
USA

ABSTRACT

FFT algorithm is one of the most applied algorithms in digital signal processing. Digital signal processing has gradually become important in biomedical application. Here hardware implementation of FFTs have found useful applications for bio-wearable devices. However, for these devices, low-power and low-area are of utmost importance. In this report, we investigate a sub-structure of decimation-in-frequency (DIF) FFT where a number of sub-bands are of interest to us. Specifically, we divide the range of frequencies into 8 sub-bands (0-7) and calculate 4 of them (1,2,5,6). We show that using concepts like *pushing* and radix 2^2, the number of complex multiplications can be drastically reduced for 16-point, 32-point and 64-point FFTs while computing those specific bands. Later, we also extend it to $N = 2^n$-point FFT based on optimized 64-point FFT structure. The number of complex multiplications is further reduced using *merge*-FFT. Our results show that the number of multiplications (and hence power) can be reduced greatly using our optimized structure compared to an unoptimized structure. This can find application in biomedical signal processing [1, 2, 3, 4, 5, 6, 7, 8] specifically while computing power spectral density of a physiological time series where reducing computational power is of utmost importance.

1. INTRODUCTION

Fast fourier transform (FFT) [9] is a widely used technique in digital signal processing. This algorithm is specifically useful for applications in telecommunications, biomedical signal processing [10, 11, 12, 13, 14, 15, 16, 17, 11, 18, 19, 20]. One of the main application of FFT based algorithms in biomedical signal processing is their usefulness in computing power spectral density (PSD). A number of methods for the computation of PSD on hardware have been proposed [21]. In these algorithms, the main bottleneck is to compute the FFT efficiently.

While computing FFT on hardware, the reduction of power and area is of utmost importance. Power consumption is directly related to number of complex multipliers in the structure. Hence, if we can reduce the number of multipliers in the hardware structure, the power consumption will also be less.

Another important observation from biomedical signal processing is that only a few of the sub-bands from available frequency range are required for computation. These bands contain most information. For example, in case of EEG data of human brain, the range of frequencies can be divided into α $(8-15\ Hz)$, β $(16-31\ Hz)$, γ $(32-50\ Hz)$, δ $(<4\ Hz)$, θ $(4-7\ Hz)$, μ $(8-12\ Hz)$ band waves. These bands relate to a number of separate physiological functions. For example, α wave indicates a relaxed, reflexive state of brain and is responsible for inhibition control. On the other hand, β band may refer to a stressed, mildly obsessive behavior. These sub-bands and their power spectral density have been shown to be useful to create biomarkers for a number of pathological conditions including prediction of seizure onset. [22].

In this report, we explore the ways to derive efficient structures for FFT when we are only concerned about a few sub-bands. Efficient FFT structures are well known in literature. Most of them use real valued signals to reduce the redundancy in architecture. Apart from that, twiddle factor transformation techniques like *pushing, modulation* and architectures like radix-$2^2, 2^3$ are also used to reduce the power consumption. We explore these transformations and use *merge-FFT* [21] to reduce number of multiplications required for computing specific sub-bands. The whole FFT band is divided into 8 sub-bands $(0-7)$. In this report, we are only concerned about computing $\{1, 2, 5, 6\}$ sub-bands. We consider the Decimation in Frequency (DIF) FFT structure for our experiment. But the same can be extended to Decimation in Time (DIT) structures as well.

The paper is structured as follows. In section 2, we revisit some techniques to reduce the number of twiddle factors. Next, in section 3 we discuss how these techniques can be used to reduce number of multiplications in computing sub-bands of 16-point, 32-point and 64-point FFTs. In section 4, we generalize our results for $N = 2^n$ point FFTs. Finally, in section 5, we further reduce the number of multiplier in FFT-structure using concepts from *merge*-FFT [21].

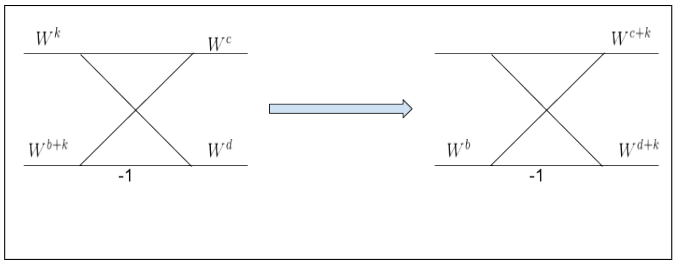

Fig. 1: Twiddle factor Pushing

2. TWIDDLE FACTOR TRANSFORMATION

The N-point discrete Fourier Transform of sequence x[n] is given by

$$X(k) = \sum_{n=0}^{N-1} x[n] W_N^{nk} \tag{1}$$

Where $W_N = e^{-j\frac{2\pi}{N}}$. For notational convenience we refer W_N^{nk} as Wk or *twiddle* factor.

2.1. Pushing

Twiddle factors can be transformed by a method called *pushing*. In this technique, a twiddle factor at the left of the butterfly diagram can be pushed to the right. This reduces the total number of twiddle factors in the FFT structure if some of the FFT points are not required for computation. We have shown this method in Fig. 1. For further clarification please refer [23].

2.2. Radix-2^k

Using FFT structure corresponding to radix-2^k can significantly reduce the number of multiplications in computation. the main idea in radix-2^k is derived from *pushing* where the twiddle factors are pushed to the right of butterfly structure. Radix-2^k means that the complex multiplications will be there after each k-stages in the FFT structure.

3. SUB-BAND CALCULATION (16-POINT, 32-POINT, 64-POINT)

In this section, we apply the previously described techniques for twiddle factor transformation in the cases of 16-point, 32-point and 64-point FFT.

3.1. 16-Point FFT

3.1.1. Single Bands

In case of 16-point *decimation in frequency* FFT structure, the FFT points corresponding to each of the 4 sub-bands {1,2,5,6} are given by $\{X(2),\ X(3)\}$, $\{X(4),\ X(5)\}$, $\{X(10),\ X(11)\}$, $\{X(12)$ and $X(13)\}$ respectively. For calculating the number of complex multiplications, we assume that twiddle factors corresponding to $1, j, -1, -j$ do not require any multiplier.

Using only *pushing*, the number of complex multiplication gets reduced by more than half while calculating either of {1,2,5,6}. In this case, bands {1,5} are similar whereas

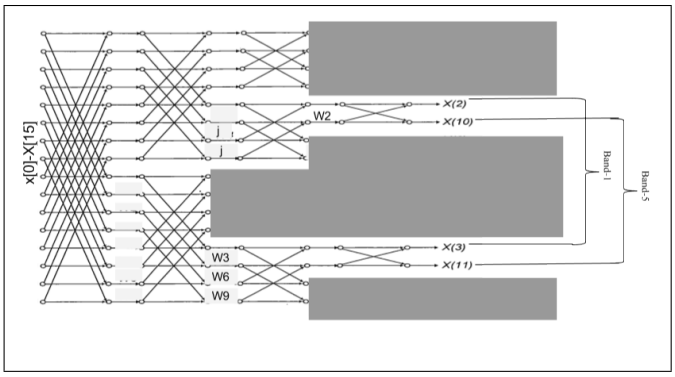

Fig. 2: Signal Flow diagram for calculating bands-1, 5

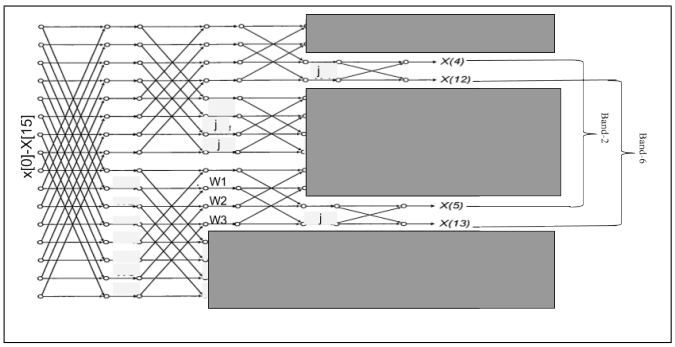

Fig. 3: Signal Flow diagram for calculating bands-2, 6

bands {2,6} are similar. We see that **Band-1** and **Band-5** require the same number of multiplications after optimization. On the other hand, **Band-2** and **Band-6** requires same number of multiplications after optimization. The signal flow diagrams are shown in Figs. 2 and 3 respectively.

- **Band-1** $X(2)$ **and** $X(3)$: Without any optimization the number of multiplications required is 10. However using transformation of twidle factors the complex multiplications is reduced to 4.
- **Band-2** $X(4)$ **and** $X(5)$: Without any optimization the number of multiplications required is 6. However using transformation of twidle factors the complex multiplications is reduced to 3.
- **Band-5** $X(10)$ **and** $X(11)$: Without any optimization the number of multiplications required is 10. However using transformation of twidle factors the complex multiplications is reduced to 4.
- **Band-6** $X(12)$ **and** $X(13)$: Without any optimization the number of multiplications required is 6. However using transformation of twidle factors the complex multiplications is reduced to 3.

3.1.2. Double Bands

When we want to compute two different bands, the minimum overlaps in terms of number of multiplications are between

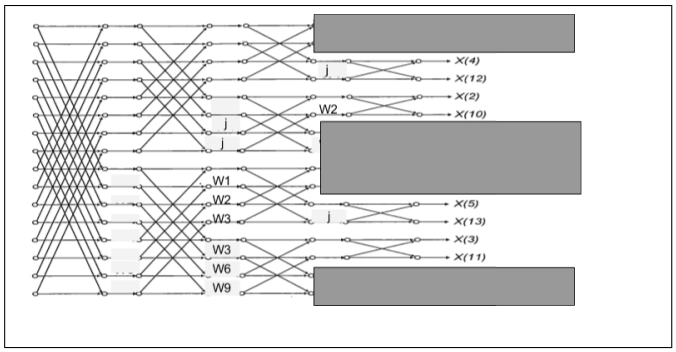

Fig. 4: Signal Flow diagram for calculating bands-1, 2, 5, 6 using *pushing*

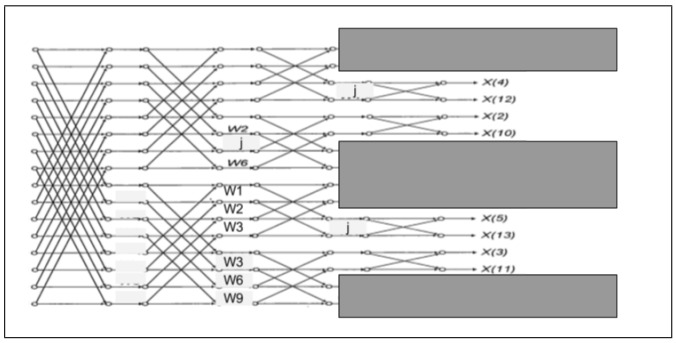

Fig. 5: Signal Flow diagram for calculating bands-1, 2, 5, 6 using 2^2

bands $1-2$, $1-6$, $2-5$ and $5-6$. The number of multiplications required for computing any of the above pair of bands is $3+4=7$. However, computing bands $1-5$ requires only 4 multiplications and computing bands $2-6$ requires 3 multiplications.

3.1.3. All Sub-Bands

The number of multipliers required is 7 in this case. The optimized signal flow diagram is shown in Fig 4.

3.1.4. Using 2^2 Structure

Here the number of multipliers required is one more than in the previous part *i.e.*, 8. The signal flow graph is shown in Fig. 5.

3.2. 32-Point FFT

Based on the optimized 16-point FFT structure, 32-point FFT structure for bands $\{1,2,5,6\}$ can be easily calculated by adding one extra stage in the beginning. In this subsection, we compare the un-optimized, 16-point optimized FFT, optimized 32-point FFT (using radix-2^2 and *pushing*) for computing the sub-bands of 32-point FFT.

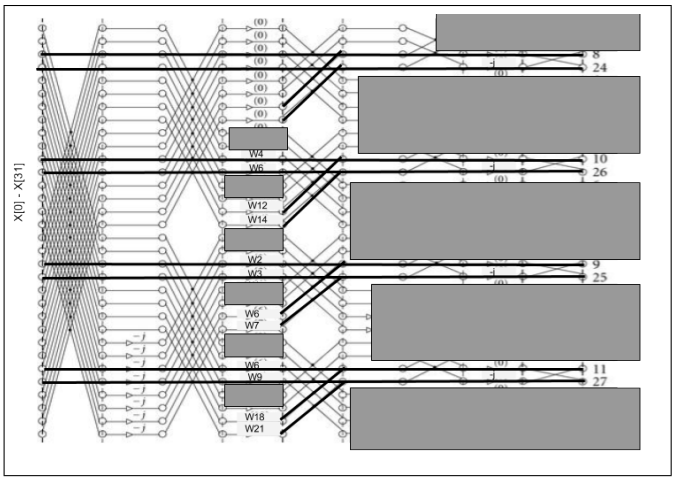

Fig. 6: Signal Flow diagram for calculating each of bands-1, 2, 5, 6 using 2^2 and *pushing*

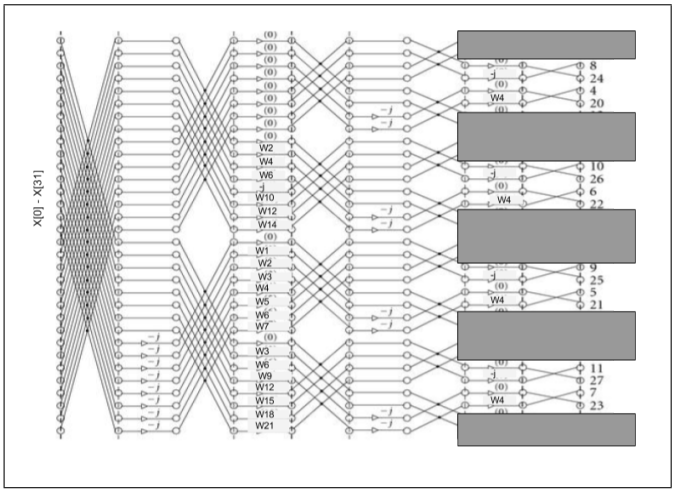

Fig. 7: Signal Flow diagram for calculating bands-1, 2, 5, 6 using 2^2 and *pushing*

3.2.1. Regular FFT Structure

For computing single and two bands, it requires 14+16 = 30 multiplications. However, to compute all of the sub-bands, the number of multipliers needed is 34

3.2.2. Extending 16-Point FFT to 32-Point FFT

To compute all of the sub-bands, number of multiplications required is $14+2\times 7=28$

3.2.3. Optimizing 32-Point FFT using 2^2 and pushing

For computing single and two bands, it requires only 12 multiplications as shown in Fig. 6. However, after optimizing, the structure itself requires 24 multiplications to calculate all of these sub-bands. This is shown in Fig. 7 In this case, both *pushing* and 2^2 result in same number of multiplications.

3.3. 64-Point FFT

In order to derive efficient structures for computing 64-point FFT sub-bands (all of {1,2,5,6}), we only use efficient structures from 16−point and 32−point. Note that we need to have 2 32-point FFT and one butterfly stage at the beginning.

3.3.1. Regular FFT Structure
The number of multipliers needed is 98

3.3.2. Extending 16-Point FFT to 64-Point FFT
Number of multiplications required is 30+ 2x28 = 86

3.3.3. Extending Optimized 32-Point FFT to 64-Point FFT
Number of multiplications required is 30+ 2x24 = 78

4. EXTENSION TO 2^N

We know that fast FFT structures require $\frac{N}{2}\log_2 N$ number of multiplications. As shown in the previous section, by using the optimized 64-point FFT structure, we only require $\frac{N}{2}[\log_2(N)-6]+78$ number of multiplications to calculate all of the {1,2,5,6} sub-bands. However, it can be noted that this is the actual upper bound of number of multipliers required. The actual number of multipliers is even less for real inputs.

We show the number of multipliers in Table. 1 and Fig. 8.

Table 1: Comparison of results

N-Point FFT	#Ms Unoptimized	#Ms Optimized
16	32	7
32	80	24
64	192	78
128	448	142
256	1024	334
512	2304	846
1024	5120	2126

5. MERGE-FFT

The number of multiplications can be further reduced for computing a large $N(=\ 2^n)$-Point FFT by using merge-FFT [21]. Suppose that we have sequences for two $N/2$ point FFTs. We can merge these two FFT sequences to create a sequence corresponding to N-Point as follows. We assume two $N/2$ point sequences are given by $X_1(k)$ and $X_2(k)$. Also, the N point sequence is given by $X(k)$. Then following [21],

$$X(2u) = X_1(u) + X_2(u) \tag{2}$$

$$X(2u+1) = X_1(u+\frac{1}{2}) - X_2(u+\frac{1}{2}) \tag{3}$$

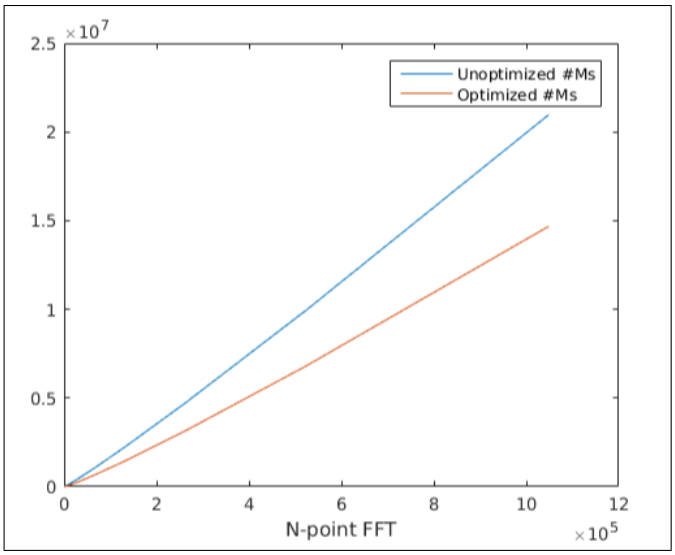

Fig. 8: Comparison between unoptimized and optimized number of multiplications to calculate all 1,2,5,6 sub-bands

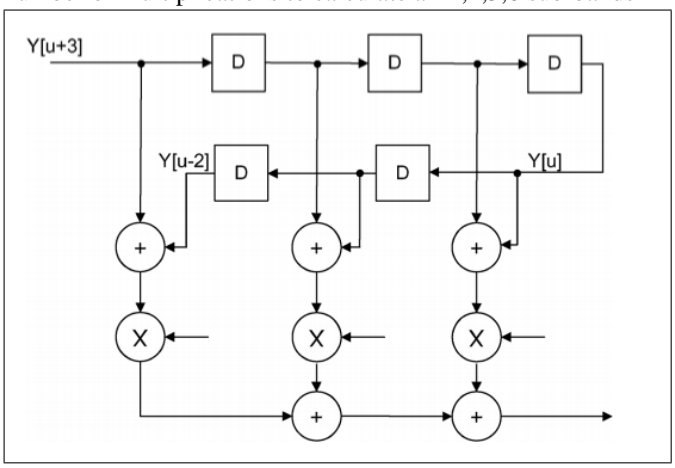

Fig. 9: Implementation of fractional delay using FIR

Implementing equation (2) does not require any multipliers. For implementing equation (3), we require a fractional delay filter of delay $D = \frac{1}{2}$. The ideal response of this filter is given by

$$h_{id}[n] = \frac{\sin(\pi(n-D))}{\pi(n-D} \tag{4}$$

Equation (5) can be implemented using an L^{th} order least-square FIR filter given by

$$h_{FIR}[n] = \ sinc(n - D + \frac{L}{2} + 1)\ 0 \leq n \leq L \tag{5}$$

In our implementation, we used $L = 6$. The filter us then given by $h_{FIR} = \{0.1273, -0.2122, 0.6366, 0.6366, -0.2122, 0.1273\}$. This a symmetric filter and can be implemented efficiently with 3 real constant multipliers. The implementation is shown in Fig. 9

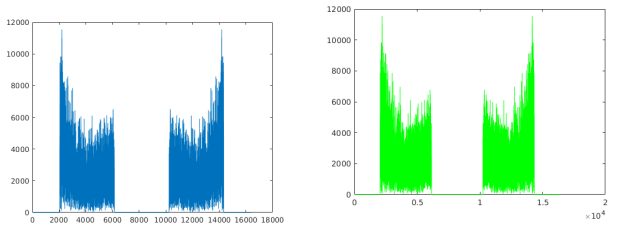

(a) Results from Optimized FFT (b) Results from Optimized FFT+*merge*-FFT

Fig. 10: Performance of Optimized FFT+*merge*-FFT for computing FFT magnitude from EEG-channel for only sub-bands $\{1,2,5,6\}$

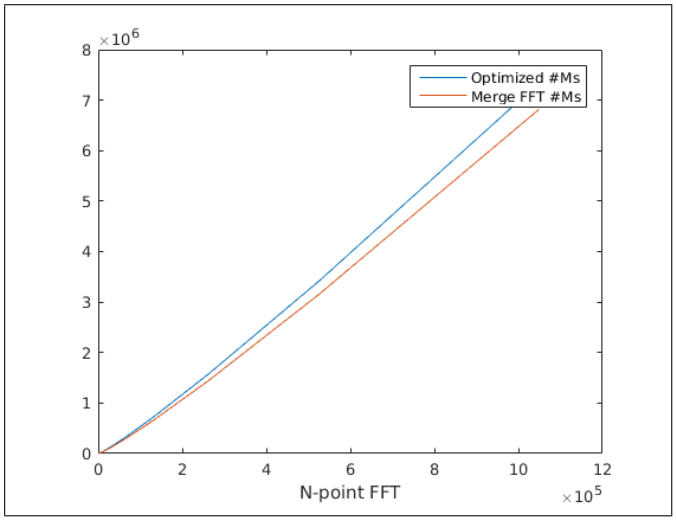

Fig. 11: Comparison between optimized number of multiplications using *pushing, radix-*2^k and optimized number of multiplications using *pushing, radix-*2^k *and merge-FFT*

5.1. Comparison of FFT for 1,2,5,6 Bands using merge-FFT

We use one EEG channel data from *kaggle* seizure prediction competition to compare the magnitude of FFT computed for bands 1,2,5,6 using merge-FFT and optimized-FFT from previous section. The result is shown in Fig. 10

5.2. Comparison between Merge-FFT and Optomized-FFT

As discussed before, using merge-FFT can replace the number of complex multipliers in the first stage using 3-constant real multipliers. Hence we only require $\frac{N}{2}[\log_2(N)-7]+78$ complex multipliers in the FFT structure to compute bands-$\{1,2,5,6\}$. The comparison between number optimized FFT multiplication and number of multiplications for merge-FFT is shown in Fig 11.

5.3. Conclusion and Future Work

In this report we performed a theoretical analysis of twiddle factor (complex multiplications) reduction while computing 4 sub-bands in case of N-point ($N=2^n$) FFTs. We derived the theoretical upper bound for the number of multipliers needed for computing the sub-bands $\{1,2,5,6\}$. In future, we plan to implement this structure in VLSI-hardware to estimate the power consumption for large N-point FFTs. This implementation will complement our theoretical analysis described in this report.

6. REFERENCES

[1] Bhaskar Sen, Neil C Borle, Russell Greiner, and Matthew RG Brown, "A general prediction model for the detection of adhd and autism using structural and functional mri," *PloS one*, vol. 13, no. 4, pp. e0194856, 2018.

[2] Bhaskar Sen, Gail A Bernstein, Tingting Xu, Bryon A Mueller, Mindy W Schreiner, Kathryn R Cullen, and Keshab K Parhi, "Classification of obsessive-compulsive disorder from resting-state fmri," in *2016 38th Annual International Conference of the IEEE Engineering in Medicine and Biology Society (EMBC)*. IEEE, 2016, pp. 3606–3609.

[3] Matthew RG Brown, James RA Benoit, Michal Juhás, Ericson Dametto, Tiffanie T Tse, Marnie MacKay, Bhaskar Sen, Alan M Carroll, Oleksandr Hodlevskyy, Peter H Silverstone, et al., "fmri investigation of response inhibition, emotion, impulsivity, and clinical high-risk behavior in adolescents," *Frontiers in systems neuroscience*, vol. 9, pp. 124, 2015.

[4] Bhaskar Sen, Shu-Hsien Chu, and Keshab K Parhi, "Ranking regions, edges and classifying tasks in functional brain graphs by sub-graph entropy," *Scientific reports*, vol. 9, no. 1, pp. 1–20, 2019.

[5] Bhaskar Sen and Keshab K Parhi, "Extraction of common task signals and spatial maps from group fmri using a parafac-based tensor decomposition technique," in *2017 IEEE International Conference on Acoustics, Speech and Signal Processing (ICASSP)*. IEEE, 2017, pp. 1113–1117.

[6] Bhaskar Sen, Gail A Bernstein, Bryon A Mueller, Kathryn R Cullen, and Keshab K Parhi, "Sub-graph entropy based network approaches for classifying adolescent obsessive-compulsive disorder from resting-state functional mri," *NeuroImage: Clinical*, vol. 26, pp. 102208, 2020.

[7] Ananda S Chowdhury, Joseph E Burns, Arka Mukherjee, Bhaskar Sen, Jianhua Yao, and Ronald M Summers,

"Automated detection of pelvic fractures from volumetric ct images," in *2012 9th IEEE International Symposium on Biomedical Imaging (ISBI)*. IEEE, 2012, pp. 1687–1690.

[8] Bhaskar Sen, Bryon Mueller, Bonnie Klimes-Dougan, Kathryn Cullen, and Keshab K Parhi, "Classification of major depressive disorder from resting-state fmri," in *2019 41st Annual International Conference of the IEEE Engineering in Medicine and Biology Society (EMBC)*. IEEE, 2019, pp. 3511–3514.

[9] J. W. Cooley and J. W. Tukey, "An algorithm for the machine calculation of complex fourier series," in *Math. Comput.*, 1965, vol. 19, pp. 297–301.

[10] Bhaskar Sen and Keshab K Parhi, "Predicting biological gender and intelligence from fmri via dynamic functional connectivity," *IEEE Transactions on Biomedical Engineering*, vol. 68, no. 3, pp. 815–825, 2020.

[11] Bhaskar Sen and Keshab K Parhi, "Predicting tasks from task-fmri using blind source separation," in *2019 53rd Asilomar Conference on Signals, Systems, and Computers*. IEEE, 2019, pp. 2201–2205.

[12] Bhaskar Sen, "Generalized prediction model for detection of psychiatric disorders," 2016.

[13] Ananda S Chowdhury, Joseph Burns, Bhaskar Sen, Arka Mukherjee, Jianhua Yao, and Ronald M Summers, "Detection of pelvic fractures using graph cuts and curvatures," in *2011 18th IEEE International Conference on Image Processing*. IEEE, 2011, pp. 1573–1576.

[14] Bhaskar Sen, Kathryn R Cullen, and Keshab K Parhi, "Classification of adolescent major depressive disorder via static and dynamic connectivity," *IEEE Journal of Biomedical and Health Informatics*, vol. 25, no. 7, pp. 2604–2614, 2020.

[15] Bhaskar Sen and Keshab K Parhi, "Constrained tensor decomposition optimization with applications to fmri data analysis," in *2018 52nd Asilomar Conference on Signals, Systems, and Computers*. IEEE, 2018, pp. 1923–1928.

[16] Bhaskar Sen and Keshab K Parhi, "Graph-theoretic properties of sub-graph entropy," *IEEE Signal Processing Letters*, vol. 28, pp. 135–139, 2020.

[17] Bhaskar Sen, Nikhil Gopal, and Xinwei Xue, "Support-bert: predicting quality of question-answer pairs in msdn using deep bidirectional transformer," *arXiv preprint arXiv:2005.08294*, 2020.

[18] Bhaskar Sen, Zheng Shi, and Gregory Burlet, "Diagnosing adhd from fmri scans using hidden markov models," *arXiv preprint arXiv:1506.06048*, 2015.

[19] Sai Sanjay Balaji, Bhaskar Sen, and Keshab K Parhi, "Effect of modulating fmri time-series on fluid ability and fluid intelligence for healthy humans," in *2021 43rd Annual International Conference of the IEEE Engineering in Medicine & Biology Society (EMBC)*. IEEE, 2021, pp. 6070–6073.

[20] Bhaskar Sen, *Static and Dynamic Connectivity Analysis of Human Brain via Functional Magnetic Resonance Imaging*, Ph.D. thesis, University of Minnesota, 2020.

[21] Keshab K Parhi and Manohar Ayinala, "Low-complexity welch power spectral density computation," *IEEE Transactions on Circuits and Systems I: Regular Papers*, vol. 61, no. 1, pp. 172–182, 2014.

[22] Yun Park, Lan Luo, Keshab K Parhi, and Theoden Netoff, "Seizure prediction with spectral power of eeg using cost-sensitive support vector machines," *Epilepsia*, vol. 52, no. 10, pp. 1761–1770, 2011.

[23] Yingjie Lao and Keshab K Parhi, "Data-canonic real fft flow-graphs for composite lengths," in *Signal Processing Systems (SiPS), 2016 IEEE International Workshop on*. IEEE, 2016, pp. 189–194.